NOTES AND CORRESPONDENCE

Circumpolar Influences on the Weddell Sea: Indication of an Antarctic Circumpolar Coastal Wave

AIKE BECKMANN AND RALPH TIMMERMANN

Alfred Wegener Institute for Polar and Marine Research, Bremerhaven, Germany

14 August 2000 and 28 February 2001

ABSTRACT

The Antarctic circumpolar wave is now a well-known feature that can be detected in atmospheric, oceanic mixed layer, and sea-ice data. In this coupled ice–ocean model driven by 40 yr of daily atmospheric forcing data, it represents a significant part of the interannual variability, linking the sea-ice and water mass formation processes in the Weddell Sea with other areas in the Antarctic water ring. In addition, these model results show a decadal-period wavelike anomaly pattern near the coast of Antarctica, propagating westward at about 2 cm s^{-1}. This coastally trapped, bottom-intensified phenomenon likely has important effects on the dense water formation rate in the Weddell Sea and even the occurrence of the Weddell polynya.

1. Introduction

Water mass transformation in the Weddell Sea is one of the sources of the global deep and bottom water. The amplitude and mechanisms of interannual and decadal changes are, therefore, of high interest for climate variability studies. A regional circumpolar coupled ice–ocean model is used to investigate the patterns, periodicities and amplitudes of fluctuations, the occurrence of single events, and possible long-term trends.

One of the prominent signals of variability in this area is the Antarctic circumpolar wave (ACW), a fluctuation with a predominantly 4-yr period, which has been suspected to also influence the deep water formation in the inner Weddell Sea (White and Peterson 1996). Comiso and Gordon (1998) pointed out that winter seasons with higher-than-normal sea-ice extent are often followed by summer seasons with lower-than-normal sea-ice extent (and vice versa) and that 4-yr periodicity can also be seen in many of the atmospheric and oceanic variables. Recently, Timmermann et al. (2001c) have quantified the influence of the ACW on deep water formation in the inner Weddell Sea by using a coupled sea-ice–ocean model and European Centre for Medium-Range Weather Forecasts data from 1985 to 1993.

The current study uses 40 yr of National Centers for Environmental Prediction–National Center for Atmospheric Research (NCEP–NCAR) reanalysis data to look at interannual and interdecadal periodicities.

2. The model

This study employs the Bremerhaven Regional Ice Ocean Simulations (BRIOS) coupled ice–ocean model as described by Timmermann et al. (2001b).

The ocean component is a terrain-following coordinate ocean circulation model (see Haidvogel et al. 1991; Song and Haidvogel 1994). The circumpolar model configuration covers the Southern Ocean south of 50°S (including the cavities beneath the major ice shelves) and has been used successfully to simulate the large-scale circulation and water mass distribution in the Weddell Sea (Beckmann et al. 1999). It is coupled to a dynamic-thermodynamic sea ice model [Hibler (1979); Lemke et al. (1990); see Timmerman et al. (2001b) for a description of the coupling]. The formulation of the ice–ocean fluxes of heat, salt, and momentum is also applied to the ice shelf base.

Previous studies with both the stand-alone ocean and the coupled ice–ocean model have concentrated on the validation of the individual model components, for example, oceanic transport measurements (Fig. 1), observed temperature–salinity (T–S) characteristics (Beckmann et al. 1999), large-scale sea-ice concentration, local sea-ice thickness, sea-ice drifter trajectories (Timmerman 2001b), and the role of sea ice in the fresh-

Corresponding author address: Dr. Aike Beckmann, Alfred Wegener Institute for Polar and Marine Research, P.O. Box 120161, D-27515 Bremerhaven, Germany.
E-mail: beckmann@awi-bremerhaven.de

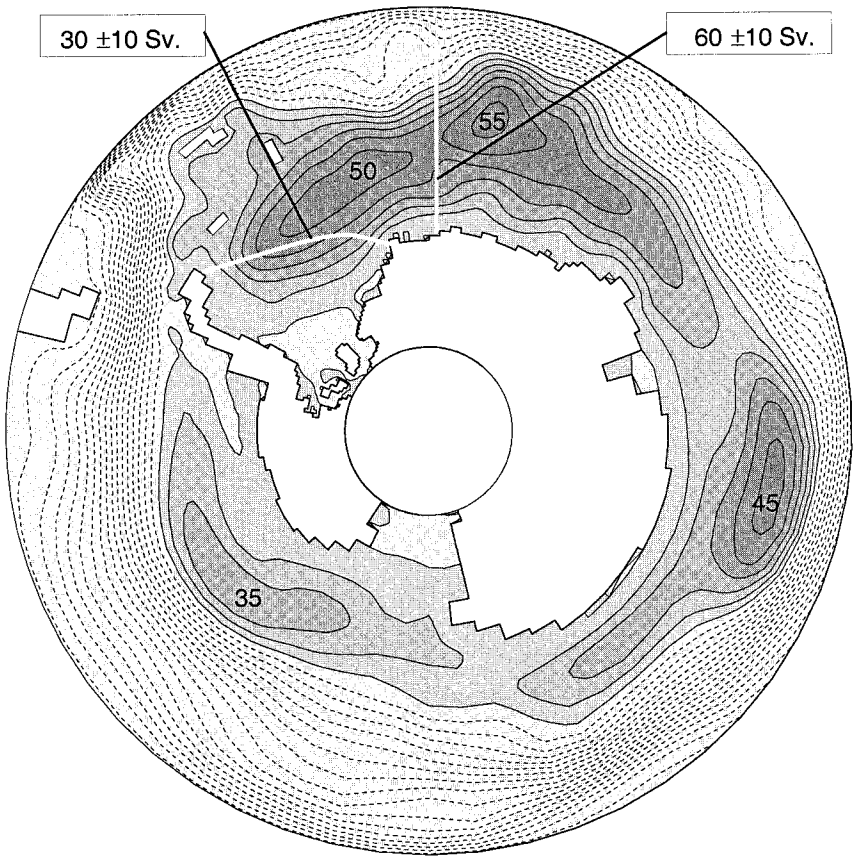

FIG. 1. Time-mean streamfunction ψ for the 40-yr NCEP–NCAR simulation ($U = -\partial\psi/\partial y$; $V = \partial\psi/\partial y$). Contour interval: 8 Sv (Sv $\equiv 10^6$ m^3 s^{-1}). The simulation shows three pronounced recirculations: the Weddell gyre (with a double-cell structure), the Kerguelen, and the Ross gyre. The Drake Passage transport is prescribed as 130 Sv. The simulated strength of the Weddell gyre has been confirmed by transport measurements along the white lines by Fahrbach et al. (1994; 30 ± 10 Sv) and Schröder and Fahrbach (1999; 60 ± 10 Sv).

water budget of the Weddell Sea (Timmermann et al. 2001a).

The experiment reported here is forced with 40 yr of NCEP–NCAR reanalysis data for the period 1958–97; two passes of the atmospheric forcing data were carried out, results from the second pass are shown. A weak drift in T–S properties away from the initial hydrography (Olbers et al. 1992) is detected through the course of the multidecadal integration, especially in the abyssal (>4000-m depth) temperatures, but was found to be significantly smaller than the interannual and interdecadal fluctuations in the coastal ocean.

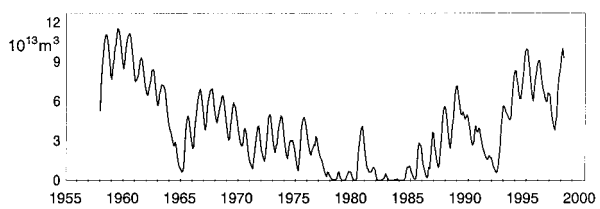

FIG. 2. Monthly mean volume of dense water (>27.9 σ_θ) in the Weddell Sea sector of the model simulation.

3. Time series of dense water volume

The main focus of this study is to investigate the interannual to interdecadal variability of dense water production in the Weddell Sea. Therefore, the central diagnostic quantity is the dense water volume (defined as water denser than 27.9 σ_θ) in the Weddell Sea sector (60°W–0°E) of the circumpolar ocean.

Figure 2 shows the temporal variation of this quantity during the 40 yr of model integration. The seasonal, interannual, and longer timescale variation in dense water volume is substantial, with dominant frequencies determined as 1.0, 4.4, and 6.7 yr (Fig. 3). In addition, there is a strong variability at the low-frequency end of the spectrum (timescales longer than 20 yr). Among these, the seasonal signal is most pronounced, and least surprising, as the dense water is formed during autumn

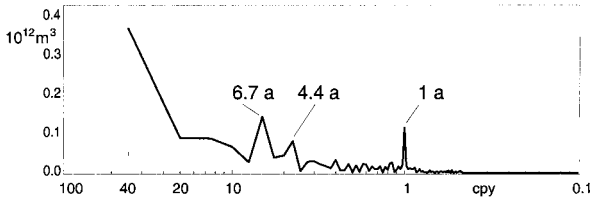

FIG. 3. Frequency spectrum of the dense water volume time series from Fig. 2.

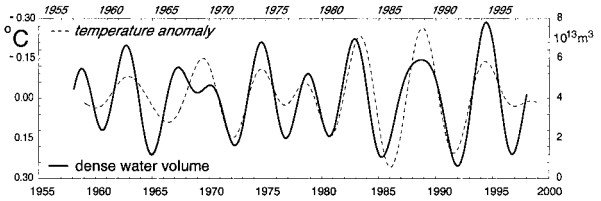

FIG. 5. Bandpass (3–7 yr)-filtered time series of dense water volume (solid line, right scale) and SST anomaly (dashed line, left scale) in the Weddell Sea sector. To enhance the visual impression of this correlation, the latter curve is plotted with a reversed vertical scale and offset by 1 yr (upper timescale).

and winter and eroded by mixing with warmer, less saline water masses during the remainder of the year.

4. Variability analysis

In this section we analyze the interannual and interdecadal modes of the variability in dense water formation in the Weddell Sea. Assuming coherent circumpolar signals, a convenient way to display these fluctuations are phase diagrams.

a. The interannual ACW signal

Beginning around 1980 (see also Bonekamp et al. 1999), fluctuations of the sea surface temperature in the Antarctic circumpolar current (ACC; 55°–65°S; Fig. 4) and sea-ice extent (not shown) exhibit the well-known eastward-propagating signal of the ACW with a 4–6 yr period (White and Peterson 1996). In our model, the anomalies tend to propagate at a mean speed of 10–15 cm s^{-1}, faster in the Indo-Pacific sector (see also Christoph et al. 1998).

Maximum amplitudes are found in the vicinity (often to the west) of the Antarctic peninsula, consistent with the assumption that the east Pacific represents the origin of these anomalies (Peterson and White 1998). The correlation between negative ACC surface temperature anomaly (averaged between 55°–65°S and 60°–0°E) and dense water volume (Fig. 5) is striking, with a notable time lag of 1 yr (cold anomaly leading dense water production). This can be explained by increased cooling and sea ice formation in the years following the cold, southerly wind anomaly phase of the ACW. It appears to be mainly caused by wind-induced northward ice export. Further studies on the mechanisms of sea ice–ocean interaction with regard to the ACW have been carried out by Timmerman et al. (2001c).

The correlation is highest in the years after 1980, indicating that the atmospheric forcing data do not con-

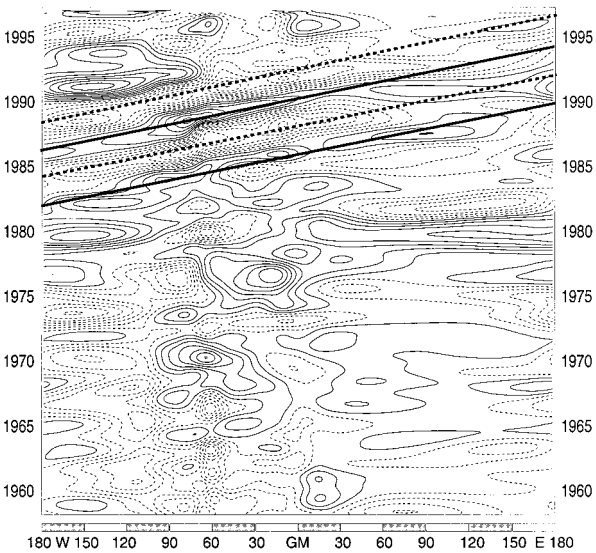

FIG. 4. Hovmöller diagram of the simulated SST anomalies in the ACC (55°–65°S) with the mean seasonal cycle removed. Solid lines denote positive values; the contour interval is 0.1 K. The straight lines represent signals 2 yr apart, traveling eastward at 11 cm s^{-1}.

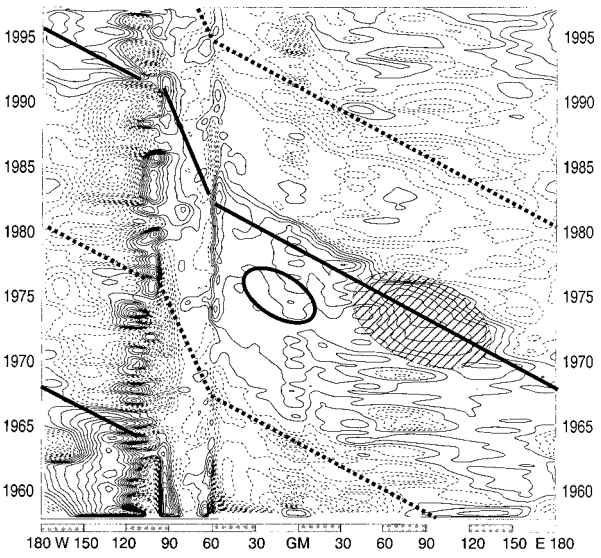

FIG. 6. Hovmöller diagram of near-coast bottom temperature. The southernmost bottom grid points are used to construct this figure. Contour interval: 0.05 K. The seasonal cycle has been removed. The shaded oval indicates the area and time of the observed Weddell polynya. The straight lines represent signals 26 yr apart, traveling westward at 2 cm s^{-1}. The hatched maximum in the early 1970s corresponds to a period of eastward surface wind anomalies in the Indian Ocean sector of the Southern Ocean.

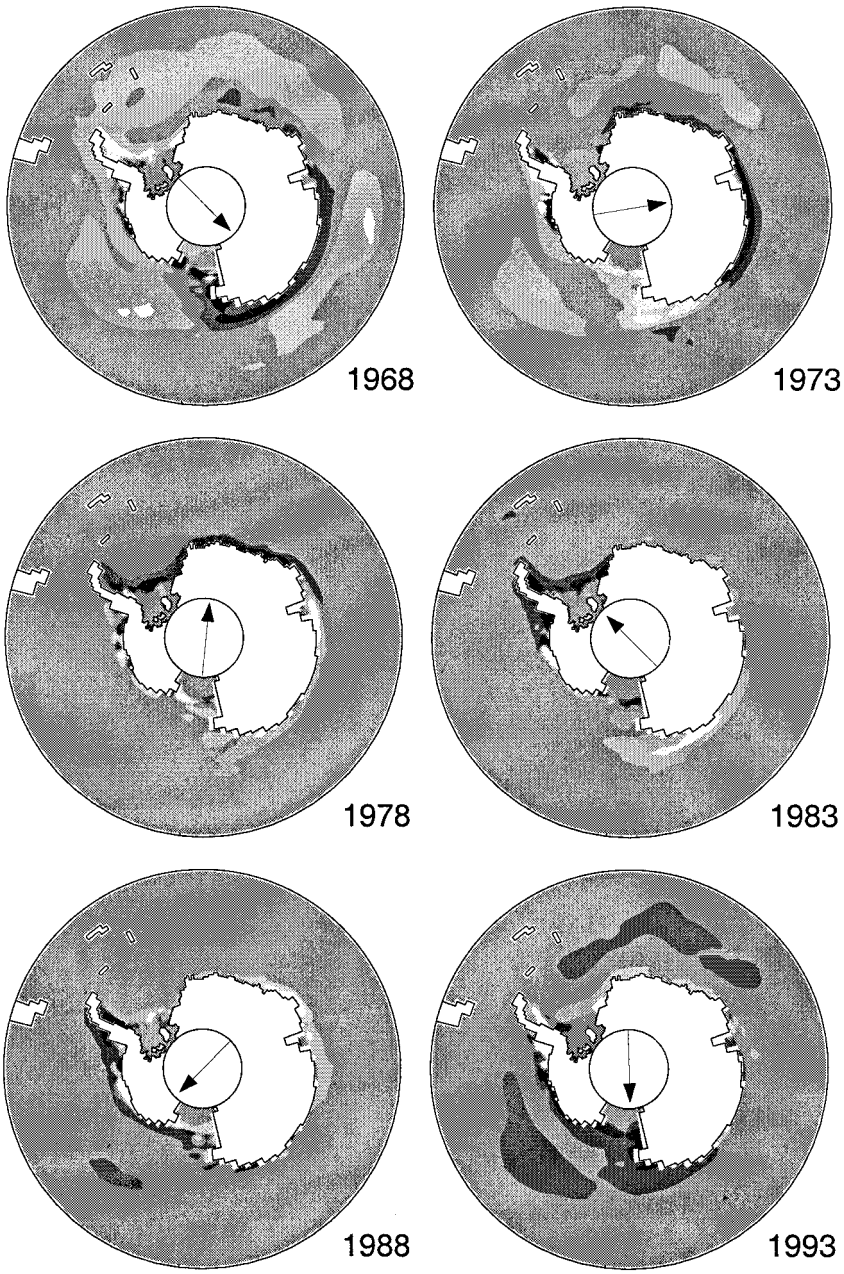

FIG. 7. Series of the distribution of Sep-mean bottom temperature. Dark (light) regions indicate warm (cold) anomalies greater than 0.1 K. The seasonal cycle has been removed. The arrows indicate the circumpolar rotation of the warm anomaly. Note that these data are not taken from a constant z level, but follow the variable bottom topography down the continental slope.

tain a coherent ACW signal in the years before. Whether this is due to the absence of the ACW prior to 1980 (which we consider unlikely) or to insufficient input data to the NCEP–NCAR models (e.g., satellite-based sea-ice concentration maps) is unknown. It is remarkable though that the 4–6-yr period is visible in both dense water volume and SST even in the years prior to 1980, even though a coherent propagating signal is missing.

b. A coherent interdecadal signal

The circumpolar nature of the ACW is in part the result of large-scale atmospheric patterns, but also due to the presence of the continuous band of eastward ocean advection between 40° and 60°S (White and Peterson 1996).

As is evident from the transport streamfunction (Fig. 1), there is another (almost) circumpolar current closer

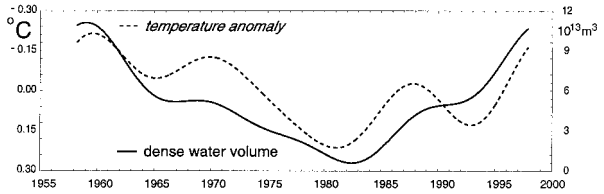

FIG. 8. Low-pass (>10 yr)-filtered time series of dense water volume (solid line, right scale) and coastal bottom temperature anomaly (dashed line, left scale) in the inner Weddell Sea (south of 70°S). As in Fig. 5, the latter curve is plotted with a reversed vertical scale.

to the continent, the Antarctic coastal current. Considering large-scale circumpolar structures that may influence the Weddell Sea's capacity of producing dense water masses, one might also look for signals traveling with this bottom-intensified westward current.

1) PHENOMENOLOGY

When looking for a temperature signal in the Antarctic coastal current, the surface signal is not well suited, as it is at freezing temperature most of the year, interrupted by brief periods of summer warming. We therefore look at the *bottom temperature variations* on the shallow continental shelf and upper slope.

The phase diagram of the near-coast bottom temperature of our simulation is shown in Fig. 6. In this presentation, a discontinuity exists at about 50°W, where (due to the north–south orientation of the coastline) a point in the inner Weddell Sea (76°S) is located right next to one at the tip of the Antarctic peninsula (65°S).

The main impression from this diagram is one of large-scale anomaly patterns with a period of about 26–30 yr. Most notable are subdecadal fluctuations of large amplitude in the Amundsen–Bellingshausen Seas (east of 90°W) and the relatively moderate variations in the inner Weddell Sea. Upon closer inspection, the temporal evolution of the bottom temperature distribution along the coast of Antarctica reveals a westward propagation with about 2–2.5 cm s^{-1}.

The three-dimensional structure of the anomaly (not shown) exhibits coastal trapping and some bottom intensification. Its lateral structure is displayed in Fig. 7, which displays September means of the bottom layer temperature anomaly at 5-yr intervals through the course of the model integration. A long-term temperature trend in the deep ocean basins (north of the ocean margin) is also visible, but relatively weak compared to the near-coastal signal.

The anomalies appear as an (imperfect) dipole around Antarctica, rotating counterclockwise around the continent. Reasons for this imperfection may be manifold: either physical (the different depth or width of the shelf, nonuniform advection by the coastal current), numerical (insufficient resolution in some crucial areas), or external (errors in atmospheric forcing data). Nevertheless, a coherent dipole structure seems to exist which, in analogy to the ACW, we call the Antarctic circumpolar coastal wave (ACCW).

The correlation of the ACCW with the dense water volume is shown in Fig. 8. The temperature maximum in the Weddell Sea in the early 1980s (Fig. 7) corresponds nicely to the simulated minimum in dense water volume (Fig. 8). It is, of course, not surprising that a positive temperature anomaly is correlated with the formation of less dense water; the main new finding, however, is that this anomaly can be traced back eastward around Antarctica and identified as a propagating and coherent disturbance on a decadal timescale.

2) MECHANISMS AND SOURCE

The detection of the ACCW anomaly pattern in our model requires an explanation of the dynamical mechanism. Its westward propagation is consistent with a 2–2.5 cm s^{-1} advection with the coastal current. An anomaly large enough to survive dissipation will advectively propagate around the continent within 25–30 yr. On the other hand, a coastal-trapped wave with circumpolar mode 2 could also have a similar phase speed. In that case, the ACCW could be interpreted as a periodic up- and downslope shift of the interface between warmer deep and colder coastal water masses. In both cases, a direct in-phase response to atmospheric forcing seems conceivable.

Even without being able to determine the propagation mechanism of the ACCW, we can look at the regional differences that might point to the generating mechanisms.

The largest variability in bottom temperature occurs on interannual timescales in the eastern Pacific sector (Fig. 6). This seems to be caused by the fluctuating summer–fall air temperatures of the NCEP–NCAR data set (not shown), which reveal largest variations in this region (see also Peterson and White 1998). This, in combination with the fact that only little information will leave the Weddell Sea westward around the Antarctic peninsula, points to the eastern Pacific as the source region for the bottom temperature anomalies, while the sink would be in the Weddell Sea.

Another notable feature is the large-scale enhancement of the amplitude in the Indian sector in the early 1970s (hatched area in Fig. 6). The forcing data for this period are characterized by a pronounced near-coast eastward surface wind anomaly. The resulting reduced downwelling at the Antarctic coast could be responsible for less downslope penetration of the cold shelf water masses.

Without further analysis, the mechanism of the ACCW must remain speculative. Further studies, analyzing both the atmospheric data and the ocean model results, are necessary.

3) CONNECTION WITH THE WEDDELL POLYNYA

As seen above, the model produces a warm anomaly at the bottom of the western and central Weddell Sea

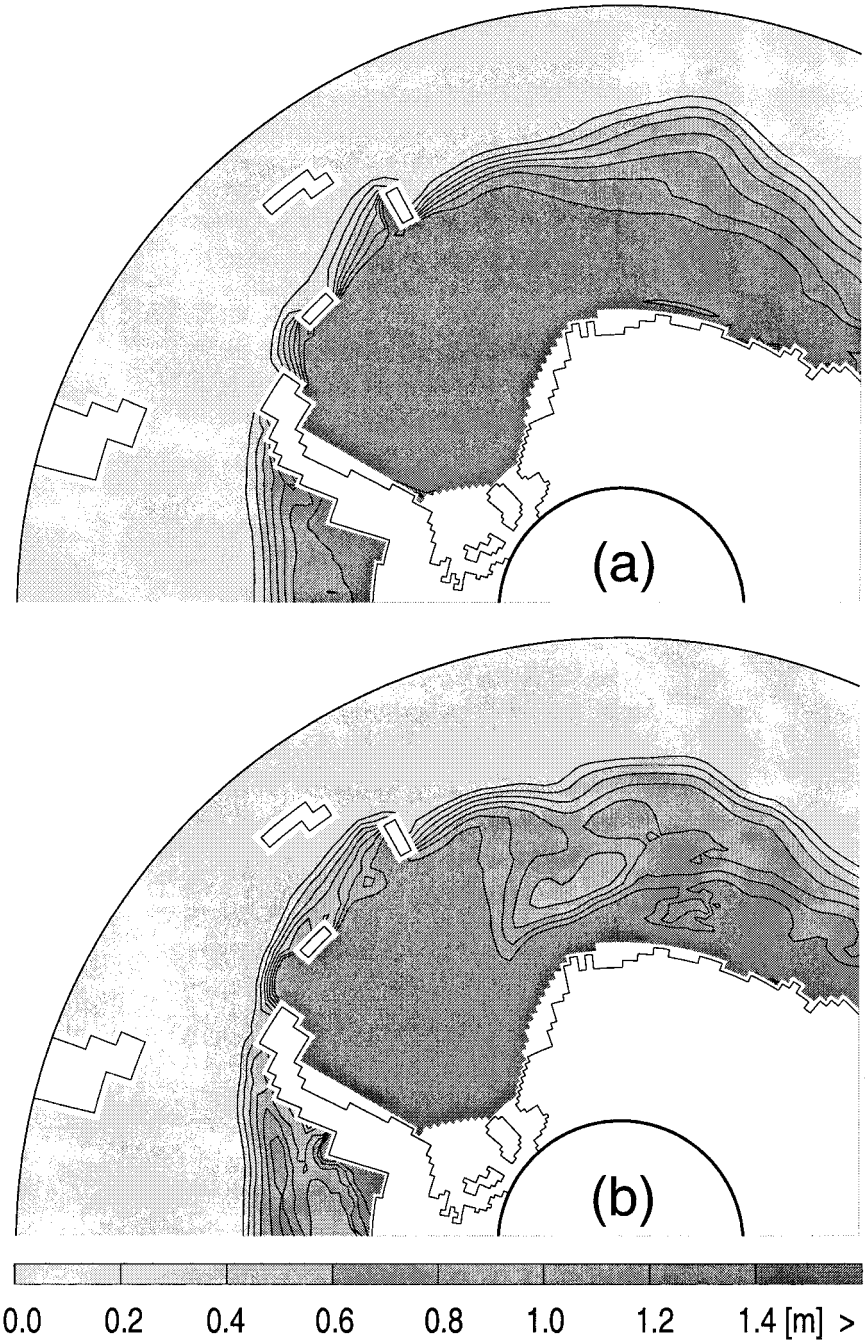

FIG. 9. Sep-mean sea-ice thickness distribution in the Weddell Sea. (a) The 40-yr climatology; (b) Sep 1975.

in the early 1980s. At the average propagation speed of 2 cm s^{-1} this maximum has passed the Greenwich meridian a few years earlier. One might suspect that the long-term variability of the ACCW seen in this model also has implications for the occurrence of the Weddell polynya, which was documented from satellite measurements in the mid-to-late 1970s (Carsey 1980).

Clearly, we cannot answer this question conclusively, as our coupled modeling system does not have sufficient resolution to explicitly include all potentially relevant processes (e.g., the details of flow around Maud Rise, other than the generation of a general doming, and some corresponding anticyclonic flow), nor does it involve an active atmosphere, which might contribute to the main-

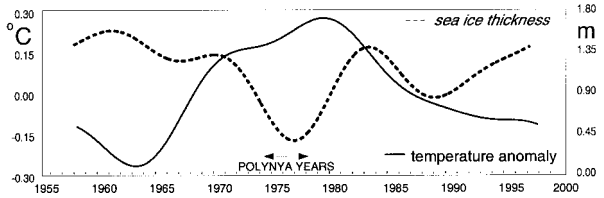

FIG. 10. Low-pass (>10 yr)-filtered bottom (3000 m) temperature (solid line, left scale) and sea-ice thickness (dashed line, right scale) west of Maud Rise (68°S, 2°W).

tenance of the Weddell polynya (Timmermann et al. 1999). However, we can have a closer look at the winter sea-ice distribution, to see if there is any effect on the sea-ice coverage during these years.

The climatological winter situation (Fig. 9a) is characterized by a continuous sea-ice cover between the continent and 60°S. The location of the northern ice edge varies a few degrees, especially in the eastern Weddell Sea, but the ice thickness distribution in the ice-covered region is rather uniform—except for two years. In 1975 (and 1976, not shown), there is a pronounced reduction of the simulated sea-ice volume west of Maud Rise (Fig. 9b). Although it would be an overstatement to call this ''a polynya,'' it is clearly a significantly reduced (by more than 50%) ice thickness. It seems plausible, that this is the model's response to the increased deep-ocean temperatures as the ACCW crest passes through the eastern Weddell Sea in the mid-to-late 1970s (Fig. 10).

Figure 10 also shows that the minimum ice thickness does not coincide with the maximum bottom temperature anomaly, in fact, the warming begins well before the decrease in sea ice. This, we believe, is the response of the coupled sea-ice–ocean system, and we hypothesize the occurrence of the Weddell polynya as follows: during the passage of a warm deep anomaly, upwelling in the Maud Rise area causes increasing temperatures also at the surface. This leads to a decrease in sea-ice thickness, modified air–sea interaction, and finally deep convection, that removes the heat from the upper- and middepth ocean. After that, sea ice will regain its usual thickness, while the bottom temperatures remain to be high for several more years, but not long enough to induce a new warming cycle. However, we believe that without higher resolution and an active atmosphere a better model representation of the Weddell polynya is hardly possible.

This scenario needs the generally enhanced upwelling at Maud Rise, but would also imply that the occurrence of the Weddell polynya might be the result of anomalies generated elsewhere around the Antarctic continent, rather than a response to the local forcing. This way, the occurrence of the Weddell polynya would be a combined effect of the large-scale situation (given by the ACCW) and the local dynamics at the isolated topography of Maud Rise.

The largest bottom temperature anomaly during the 1970s occurred farther east, in the eastern Indian sector of the Southern Ocean (60°–120°E, see Fig. 6). As pointed out before, the eastward wind anomaly in the Indian sector of the coastal Southern Ocean might be important in this respect. It then seems plausible that persistent atmospheric blocking situations may play a role in strengthening oceanic bottom temperature anomalies through their wind field.

5. Summary and conclusions

Using a circumpolar coupled ice–ocean model, we have looked at the interannual and interdecadal variability in dense water formation in the Weddell Sea. We have found and confirmed a correlation with the ACW, on a roughly 4-yr timescale. At the same time, a much longer variation was detected in the experiment with NCEP–NCAR reanalysis atmospheric forcing. Upon closer inspection, this variability seems to be related to the passage of a bottom-intensified, coastal-trapped temperature anomaly.

We conclude, that the Weddell Sea dense water formation anomalies are correlated with the following:

- the passage of the ACW (maximum formation one year after strong southerly winds) on a 4–6-yr periodicity; and
- the passage of the ACCW (minimum formation during warm anomalies) on a 26–30-yr periodicity.

We also speculate that the occurrence of the Weddell polynya is related to the passage of the ACCW, through upwelling of anomalous warm water. This is a new hypothesis, in that it assumes nonlocal (circumpolar) rather than local causes for the occurrence of the Weddell polynya (as suggested, e.g., by Gordon and Huber 1984; Martinson 1990) and also points to a long-term periodicity of this apparently singular phenomenon. Last, we note that the terrain-following coordinate of the ocean model is especially well suited for the simulation of the propagation of topographic waves and near-bottom structures along coastal boundaries.

6. Outlook

The pronounced periodicity and relatively regular propagation of the ACCW suggests robust predictive skills with respect to this phenomenon. However, a prediction of the next occurrence of the Weddell polynya based on the results of our coupled ice–ocean model is tempting but would be premature. Too little is known about the physical and numerical sensitivities of this phenomenon, its interaction with the ACW, as well as the quality of the atmospheric data.

Still, a linear extrapolation of our model ACCW into the future indicates that there should be another warm signal in the eastern Weddell Sea around 2005. Its actual amplitude, however, will probably be determined right now by processes farther east (60°–120°E), including Prydz Bay, an area the model identifies as crucial for

air–sea interaction and Antarctic dense water formation (Schodlok et al. 2001).

Acknowledgments. Helpful discussions with Hartmut Hellmer and other members of the BRIOS team are gratefully acknowledged. Special thanks go to Christoph Lichey for processing the atmospheric forcing data for use in the BRIOS modeling system. Comments by D. Martinson and an anonymous reviewer helped to improve the manuscript. The NCEP atmospheric forcing fields were received via the NOAA–CIRES Climate Diagnostics Center, Boulder, Colorado, using the Web site http://www.cdc.noaa.gov/.

REFERENCES

Beckmann, A., H. H. Hellmer, and R. Timmermann, 1999: A numerical model of the Weddell Sea: Large scale circulation and water mass distribution. *J. Geophys. Res.,* **104,** 23 375–23 391.

Bonekamp, H., A. Sterl, and G. J. Komen, 1999: Interannual variability in the Southern Ocean from an ocean model forced by European Centre for Medium-Range Weather Forecasts reanalysis fluxes. *J. Geophys. Res.,* **104,** 13 317–13 331.

Carsey, F. D., 1980: Microwave observations of the Weddell polynya. *Mon. Wea. Rev.,* **108,** 2032–2044.

Christoph, M., T. P. Barnett, and E. Roeckner, 1998: The Antarctic circumpolar wave in a coupled ocean–atmosphere GCM. *J. Climate,* **11,** 1659–1672.

Comiso, J. C., and A. L. Gordon, 1998: Interannual variability in summer sea ice minimum, coastal polynyas and bottom water formation in the Weddell Sea. *Antarctic Sea Ice: Physical Processes, Interactions and Variability,* M. O. Jeffries, Ed., Antarctic Research Series, Vol. 74, Amer. Geophys. Union, 293–315.

Fahrbach, E., G. Rohardt, M. Schröder, and V. Strass, 1994: Transport and structure of the Weddell gyre. *Ann. Geophys.,* **12,** 840–855.

Gordon, A. L., and B. A. Huber, 1984: Thermohaline stratification below the southern ocean sea ice. *J. Geophys. Res.,* **89,** 641–648.

Haidvogel, D. B., J. L. Wilkin, and R. E. Young, 1991: A semi-spectral primitive equation ocean circulation model using vertical sigma and orthogonal curvilinear horizontal coordinates. *J. Comput. Phys.,* **94,** 151–184.

Hibler, III, W. D., 1979: A dynamic-thermodynamic sea ice model. *J. Phys. Oceanogr.,* **9,** 815–846.

Lemke, P., W. B. Owens, and W. D. Hibler III, 1990: A coupled sea ice–mixed layer–pycnocline model for the Weddell Sea. *J. Geophys. Res.,* **95,** 9513–9525.

Martinson, D. G., 1990: Evolution of the Southern Ocean winter mixed layer and sea ice; open ocean deep water formation and ventilation. *J. Geophys. Res.,* **95,** 11 641–11 654.

Olbers, D. J., V. Gouretski, G. Seiß, and J. Schröter, 1992: *Hydrographic Atlas of the Southern Ocean.* Alfred Wegener Institute, 82 pp.

Peterson, R. G., and W. B. White, 1998: Slow oceanic teleconnections linking the Antarctic circumpolar wave with the tropical El Niño–Southern Oscillation. *J. Geophys. Res.,* **103,** 24 573–24 583.

Schodlok, M. P., C. Rodehacke, H. H. Hellmer, and A. Beckmann, 2001: On the origin of the deep CFC maximum in the eastern Weddell Sea—numerical model results. *Geophys. Res. Lett.,* in press.

Schröder, M., and E. Fahrbach, 1999: On the structure and the transport of the eastern Weddell gyre. *Deep-Sea Res.,* **46,** 501–527.

Song, Y., and D. B. Haidvogel, 1994: A semi-implicit ocean circulation model using a generalized topography-following coordinate. *J. Comput. Phys.,* **115,** 228–244.

Timmermann, R., P. Lemke, and C. Kottmeier, 1999: Formation and maintenance of a polynya in the Weddell Sea. *J. Phys. Oceanogr.,* **29,** 1251–1264.

——, A. Beckmann, and H. H. Hellmer, 2001a: The role of sea ice in the fresh water budget of the Weddell Sea. *Ann. Glaciol.,* **33,** in press.

——, ——, and ——, 2001b: Simulation of ice–ocean dynamics in the Weddell Sea. Part I: Model description and validation. *J. Geophys. Res.,* in press.

——, H. H. Hellmer, and A. Beckmann, 2001c: Simulation of ice–ocean dynamics in the Weddell Sea. Part II: Interannual variability 1985–1993. *J. Geophys. Res.,* in press.

White, W. B., and R. G. Peterson, 1996: An Antarctic circumpolar wave in surface pressure, wind, temperature and sea ice extent. *Nature,* **380,** 699–702.